Molecular Therapy
Nucleic Acids
Original Article

In vivo base editing of Angptl3 via lipid nanoparticles to treat cardiovascular disease

Jennifer Khirallah,[1,8] Hanan Bloomer,[1,2,8] Douglas Wich,[1] Changfeng Huang,[1] J. Noah Workman,[3] Yamin Li,[1] Gregory A. Newby,[3,4,5,6,7] David R. Liu,[5,6,7] and Qiaobing Xu[1,2]

[1]Department of Biomedical Engineering, Tufts University, Medford, MA 02155, USA; [2]School of Medicine and Graduate School of Biomedical Sciences, Tufts University, Boston, MA 02111, USA; [3]Department of Genetic Medicine, Johns Hopkins University, Baltimore, MD 21205, USA; [4]Department of Biomedical Engineering, Johns Hopkins University, Baltimore, MD 21218, USA; [5]Merkin Institute of Transformative Technologies in Healthcare, Broad Institute of MIT and Harvard, Cambridge, MA 02142, USA; [6]Department of Chemistry and Chemical Biology, Harvard University, Cambridge, MA 02138, USA; [7]Howard Hughes Medical Institute, Harvard University, Cambridge, MA 02138, USA

Cardiovascular disease (CVD) is the leading cause of death globally and is exacerbated by elevated blood levels of low-density lipoprotein cholesterol (LDL-C) and triglycerides (TGs). Existing approaches for decreasing blood lipid levels rely on daily medications, leading to poor patient adherence. Gene therapy represents a promising "one and done" strategy to durably reduce blood lipid levels. *ANGPTL3* has emerged as a potential target for gene therapy, as naturally occurring loss-of-function variants are cardioprotective. Here, we use lipid nanoparticles to package and deliver CRISPR adenine base editors (ABEs), which enable gene knockout without requiring potentially harmful DNA double-strand breaks. We package ABE mRNA and a synthetic guide RNA targeted to disrupt an important splice site in *Angptl3*, which we administered to mice intravenously. We achieved over 60% base editing in the liver and durable reductions in serum ANGPTL3, LDL-C, and TGs for at least 100 days. Notably, blood lipid levels remained low when mice were challenged with a high-fat high-cholesterol diet up to 191 days after therapy. These results provide a foundation for a potential one-and-done treatment for CVD.

INTRODUCTION

Cardiovascular disease (CVD) encompasses a range of conditions affecting the circulatory system, which comprises the heart and the vasculature responsible for the transportation of blood throughout the body. As the leading cause of death worldwide, CVD remains a significant global health concern. The incidence of CVD is growing annually, exacerbated by lifestyle changes such as an increase in sedentary or remote jobs, a decrease in physical activity, and higher calorie diets with more saturated fats.[1,2] Elevated levels of cholesterol and/or fats in the blood can lead to the development of atherosclerosis, thereby increasing the risk of CVD in patients. Current treatment options for CVD, including chronic medications (e.g., statins) and lifestyle changes, face challenges in patient adherence, partly due to the daily dosing of medication and constant need for managing exercise and dietary habits.

Gene therapy offers a unique opportunity to create a one-and-done therapy for patients by durably reducing blood cholesterol and fats.[3,4] The gene, encoding angiopoietin-like 3 (ANGPTL3), a protein that regulates plasma lipoprotein levels, has been identified as a candidate target for treating dyslipidemia-related diseases. ANGPTL3 is primarily expressed by liver hepatocytes and is secreted into the bloodstream, where it inhibits enzymes involved in cholesterol and triglyceride (TG) metabolism, leading to increased plasma lipid levels.[5] Loss of function (LOF) variants of *ANGPTL3* are naturally occurring in the human population with no known associated complications.[6–8] Individuals with these mutations have shown reduced levels of plasma low-density lipoprotein cholesterol (LDL-C) and TGs, as well as protection against CVD.[7,8] Efforts to inhibit ANGPTL3 for CVD treatment are ongoing, using antisense oligonucleotides, short interfering RNA, and monoclonal antibodies.[9–12] However, these approaches suffer from similar limitations to existing therapies, such as temporary therapeutic effects that require regular redosing. We rationalized that inducing a LOF mutation in *ANGPTL3* represents a more precise and durable strategy for reducing ANGPTL3 levels and may confer protection against CVD.

Received 28 February 2024; accepted 12 February 2025;
https://doi.org/10.1016/j.omtn.2025.102486.

[8]These authors contributed equally

Correspondence: Gregory A. Newby, Department of Genetic Medicine, Johns Hopkins University, Baltimore, MD 21205, USA.
E-mail: gnewby@jhmi.edu
Correspondence: David R. Liu, Merkin Institute of Transformative Technologies in Healthcare, Broad Institute of MIT and Harvard, Cambridge, MA 02142, USA.
E-mail: dliu@broadinstitute.org
Correspondence: Qiaobing Xu, Department of Biomedical Engineering, Tufts University, Medford, MA 02155, USA.
E-mail: qiaobing.xu@tufts.edu

Generating an LOF mutation in *ANGPTL3* may be achieved with *in vivo* genome editing. The CRISPR-Cas system has emerged as a powerful genome editing tool that enables precise genetic changes.[13,14] Cas nucleases, such as Cas9, generate a DNA double-strand break (DSB) at a target sequence, which can be repaired by non-homologous end-joining or homology-direct repair. Previously, we used CRISPR-Cas9 to generate indels within exon 1 of *Angptl3* in mice, leading to a functional gene knockout.[15] Cas9 mRNA and a single guide RNA (sgRNA) were packaged in a liver-targeting lipid nanoparticle (LNP) and delivered to mice via tail vein injection. We achieved editing of approximately 35% in the liver and a significant reduction in serum ANGPTL3, LDL-C, and TG for up to 100 days.

While this technique offers a promising strategy, DSBs generated by Cas nucleases are of significant concern due to the potential for complex deletions, translocations, and chromosomal rearrangements, which could lead to oncogenic transformation.[16–18] Moreover, DSBs can initiate a cascade of internal signaling that leads to p53-mediated cell-cycle arrest or apoptosis.[19–22] Recently, CRISPR base editors (BEs) were shown to induce single nucleotide modifications with minimal DSB byproducts.[23–25] BEs contain a catalytically impaired nickase Cas9 fused to an engineered deaminase enzyme, which catalyzes a substitution reaction within a five-base activity window. Notably, BEs can disrupt genes by inactivating splice acceptor and splice donor sites at the intron-exon junctions.[26] We thus rationalized that using CRISPR BEs could represent a safer approach to knockout *Angptl3*.

Successful delivery of BE mRNA and sgRNAs to the liver signifies a critical step for our one-time *in vivo* therapy. Previous studies targeting *Angptl3* for gene therapy use adeno-associated virus (AAV) vectors.[27,28] However, LNPs offer advantages over AAV as a delivery system, such as reduced immunogenicity, greater packaging capacity, transient expression of BEs, and targeted organ delivery.[29,30] Here, we describe the use of liver-targeting LNPs for the delivery of adenine base editor (ABE) mRNA and sgRNAs targeting *Angptl3* splice sites in mice as a potential treatment for CVD.

RESULTS

sgRNA and LNP design enables efficient *in vivo* base editing of *Angptl3* in mice

We hypothesized that disrupting the highly conserved splice acceptor (AG dinucleotide at the 3′ end of an intron) or splice donor (GT dinucleotide at the 5′ end of an intron) sites in the mouse *Angptl3* gene would result in a functional knockout and decreased plasma lipid levels. All possible ABE sgRNAs targeting splice sites were considered and assessed for the presence of homologous protospacer adjacent motif (PAM) sites in the human *ANGPTL3* gene, which would improve clinical translatability. Based on these criteria, we identified two candidate sgRNAs disrupting the exon 6 splice acceptor (sgAngptl3_SA) and splice donor (sgAngptl3_SD) sites (Figure 1A). Given the protection against CVD conferred by naturally occurring LOF mutations in exons 6 and 7 of the human *ANGPTL3* locus, we hypothesized that disrupting the splice sites at exon 6 using ABEs represents a viable approach for achieving gene knockout.[12,31] For both sgRNAs, conversion of the adenine in position 6 (A6) of the protospacer sequence to guanine (as predicted), thymine, or cytosine, results in disruption of the key splice recognition sites (Figure 1A).

Second, we wanted to screen multiple lipids for our liver-targeting gene editing application. Our lab recently synthesized two novel lipids, lipid 88 (L88) and lipid 10 (L10), predicted to enable efficient liver targeting (Figure 1B). We have previously demonstrated that LNPs formulated with L88 enabled delivery of mRNA to the mouse liver after intramuscular injection.[32] To test the ability of these new lipids to delivery mRNA to the mouse liver after intravenous (IV) injection, LNPs were formulated with L88, L10, and 306-O12B, a lipid that previously enabled *in vivo* Cas9-mediated knockout of *Angptl3* in the mouse liver, and packaged with Firefly luciferase (FLuc) mRNA. At 6 h after tail vein injection of LNPs into mice, L88 demonstrated a significant increase in total radiance in the liver compared with 306-O12B and L10 (Figure 1C). Next, to test whether our lipids could mediate base editing in the mouse liver, LNPs were packaged with ABE8e mRNA and either sgAngptl3_SA or sgAngptl3_SD and administered into 6- to 8-week-old C57BL/6J mice via tail vein injection at a total RNA dose of 3 mg/kg. After 7 days, livers were harvested for next-generation sequencing (NGS) and analyzed at the target site. LNPs formulated with L88 exhibited robust disruption of the splice site with efficiencies of 39.6% and 64% using sgAngptl3_SA and sgAngptl3_SD, respectively (Figure 1D). In contrast, formulations with L10 yielded editing rates of 26.1% and 47.5% for sgAngptl3_SA and sgAngptl3_SD, respectively (Figure 1D). Due to the improved delivery of FLuc mRNA to the liver with L88 and higher average base editing with L88 across both sgRNAs, we selected it as the active lipid for LNP formulation in all remaining experiments.

In vivo base editing with splice donor targeting sgRNA achieves high editing efficiency and minimal indel formation

LNPs were formulated with L88 and loaded with ABE8e mRNA and either sgAngptl3_SA (denoted LNP_SA) or sgAngptl3_SD (denoted LNP_SD) and delivered at a total RNA dose of 3 mg/kg. Before injection into mice, the zeta potential and effective diameter of the formulated LNPs were measured. LNP_SA had an average effective diameter of 103.1 nm, a polydispersity index (PDI) of 0.21, and a zeta potential of −9.3 mV, whereas LNP_SD had an average effective diameter of 131.4 nm, a PDI of 0.24, and a zeta potential of −3.9 mV (Table S1).

Seven days after tail vein injection into C57BL/6J mice, livers were harvested for detailed NGS analysis. We found that total editing at the A6 position was 63.1% for LNP_SA and 64.6% for LNP_SD (Figure 2A). A high purity of A-to-G conversions was observed, accounting for more than 95% and 99% of edits at A6 with LNP_SA and LNP_SD, respectively (Figures S1A and S1B). Given our approach of targeting splice sites to disrupt *Angptl3*, rather than precisely correcting specific pathogenic mutations, A-to-T and A-to-C edits are not detrimental and still result in gene knockout. Bystander edits were observed at adenines located between positions 4 and 14 within

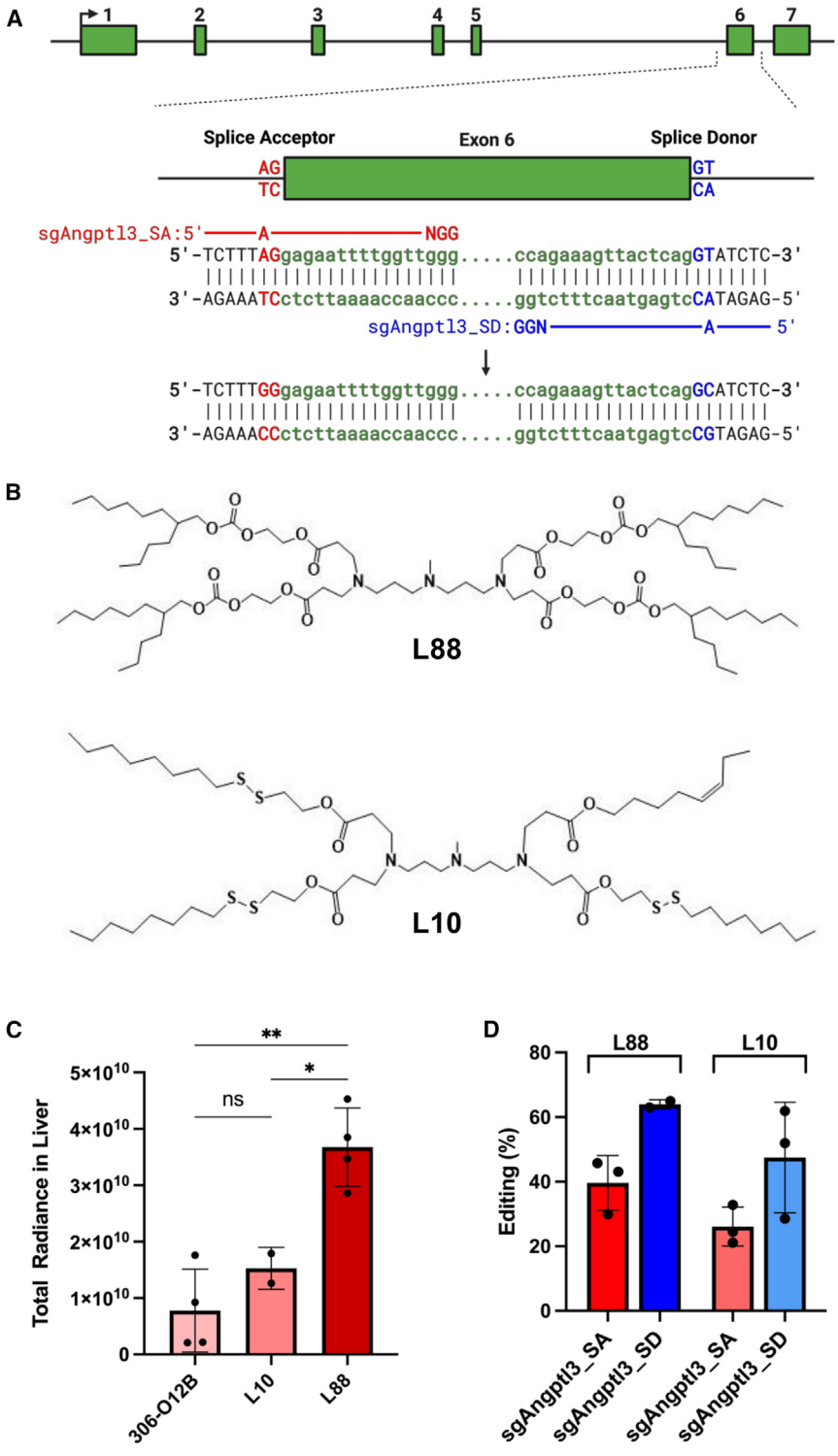

Figure 1. sgRNA design and LNP formulation facilitate efficient *in vivo* base editing of *Angptl3* in mice

(A) Schematic showing the mouse *Angptl3* locus. Both the mouse and human *Angptl3* gene are composed of 7 exons (green). The highly conserved splice acceptor (SA) site (AG dinucleotide at the 3′ end of the intron, red) of exon 6 can be disrupted using sgAngptl3_SA (red), which converts the adenine (A) at position 6 of the protospacer on the sense strand to a guanine (G). Alternatively, the splice donor (SD) site (GT dinucleotide at the 5′ end of the intron, blue) of Exon 6 can be disrupted using sgAngptl3_SD (blue), which converts the A at position 6 of the protospacer on the anti-sense strand to a G, resulting in a cytosine (C) on the sense strand. NGG refers to the PAM sequences. (B) Chemical structure of L88 (top) and L10 (bottom). (C) Total radiance observed in the mouse liver via an IVIS imaging system 6 h after IV injection with LNPs formulated with lipid 306-O12B, L10, or L88, and packaged with FLuc mRNA (n = 2–4). (D) Total editing in mouse livers 7 days after administration of LNPs formulated with L88 or L10 and coloaded with ABE8e mRNA and either sgAngptl3_SA or sgAngptl3_SD (n = 2–3). Results displayed as mean ± standard deviation. Significance determined by one-way ordinary ANOVA. $^{*}p < 0.05$, $^{**}p < 0.01$.

the protospacer sequence (Figures S1C and S1D). However, as bystander edits are not expected to interfere with the splice disruption caused by editing of the target adenine at position 6, these edits do not compromise the intended outcome. Importantly, we observed minimal indels at the target loci for both LNP_SA and LNP_SD. LNP_SA exhibited a 3.34% indel rate with an editing-to-indel ratio of 19.6, while LNP_SD resulted in a lower indel rate of 1.47% and a higher editing-to-indel ratio of 44.2 (Figures 2B and 2C). This suggests that LNP_SD has a safer therapeutic profile by mitigating the risks associated with DNA DSB generation. The liver is composed of approximately 60%–70% hepatocytes, and editing up to 70% has been achieved with adenine BEs (ABEs).[3,4] To determine if we could improve base editing efficiencies in the liver to 70%, mice were administered either one or two doses of 3 mg/kg LNPs, with a 48-h interval between doses. Rothgangl et al.[4] demonstrated that a double dose regimen can significantly increase *in vivo* base editing efficiencies. We found no significant differences in editing levels between mice receiving a single or double dose of LNP_SA or LNP_SD (Figure 2D). This suggests that we achieved maximum editing at our loci at approximately 60% with our LNP formulations. Based on these results, future studies used a single dose of 3 mg/kg LNPs, which allows for optimal editing efficiencies while limiting any potential toxicity associated with multiple LNP doses. Finally, to ensure that

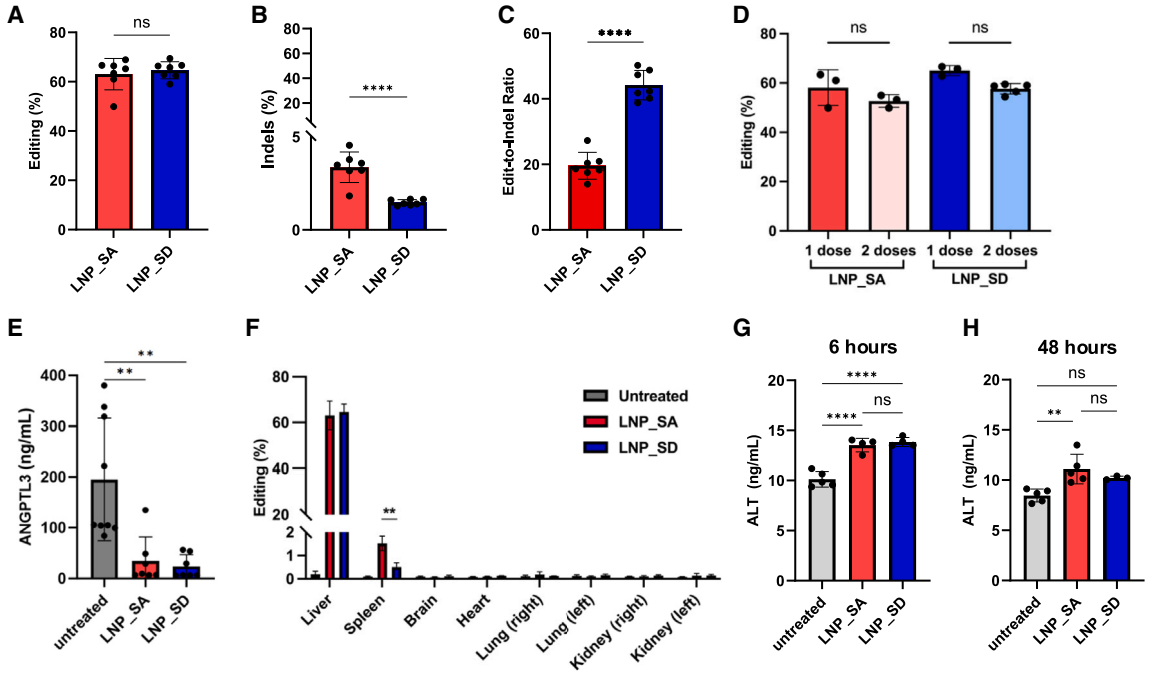

Figure 2. Efficient *in vivo* base editing at *Angptl3* with minimal indels and a favorable safety profile

(A) Total editing in mouse livers 7 days after administration of LNP_SA or LNP_SD (LNPs formulated with L88 and co-loaded with ABE8e mRNA and either sgAngptl3_SA or sgAngptl3_SD) ($n = 7$). (B) Insertions and/or deletions (indels) at target loci 7 days after LNP administration ($n = 7$). (C) Total editing (A) to indel (B) ratio after 7 days ($n = 7$). (D) Total editing in mouse livers after administration of 1 or 2 doses of 3 mg/kg LNPs. Second dose was given 48 h after the first dose and analysis was completed 7 days after the first dose ($n = 3$–5). (E) Serum levels of ANGPTL3 7 days after LNP administration ($n = 7$–9). (F) Total editing in six different organs 7 days after LNP administration ($n = 7$–10). (G and H) ALT at (G) 6 h ($n = 4$–5) and (H) 48 h ($n = 3$–5) after administration of LNPs.

Results displayed as mean ± standard deviation. Significance determined by unpaired student's T test for (A), (B), (C), and (D), and with one-way ordinary ANOVA for (E), (F), (G), and (H). $^{**}p < 0.01$, $^{****}p < 0.0001$.

base editing led to a reduction in ANGPTL3 levels, serum ANGPTL3 was measured 7 days after IV injection of LNPs into mice. We observed a greater than 90% decrease in serum ANGPTL3 with both LNP_SA and LNP_SD (Figure 2E).

LNPs packaged with splice donor targeting sgRNA enables a safer therapeutic design

Achieving high tissue tropism is critical for ensuring the safety of genome editing therapies. Our lab and others have shown that certain LNPs are able to target the liver with high specificity.[33] To determine the ability for LNPs formulated with L88 to deliver base editing apparatus with hepatotropism, editing frequencies were assessed in six different organs. We found that the liver was the predominant site of on-target editing for both LNP_SA and LNP_SD (Figure 2F). While editing in the spleen was significantly lower than in the liver for both formulations, LNP_SD treated mice exhibited a reduced spleen editing rate of 0.5% compared with 1.5% in LNP_SA treated mice. We found that editing rates in the brain, heart, lung, and kidney were less than 0.2% for both LNP_SA and LNP_SD, consistent with untreated controls and representative of baseline NGS error. To determine the off-target activity for our *Angptl3*-targeting sgRNAs, we performed an *in silico* prediction of potential off-target sites using Cas-OFFinder. For both sgAngptl3_SA and sgAngptl3_SD, no DNA off-target sites were identified with 1 or 2 mismatches to the protospacer sequence. For sgAngptl3_SA, 20 sites were identified with 3 mismatches, whereas for sgAngptl3_SD, 7 sites were identified with 3 mismatches (Tables S2 and S3). PCR amplification and NGS analysis of these potential off-target sites was performed. Five of the 20 sgAngptl3_SA and 1 of the 7 sgAngptl3_SD off-target sites failed to specifically amplify, likely due to their location within repetitive sequences. Of the 15 successfully amplified potential off-target loci for sgAngptl3_SA, we observed a significant increase in A-to-G editing at one site, off-target site 10 (OT10_SA), where editing rates increased by 5.29% in LNP_SA-treated mice (Figure S2A). Two of the 15 predicted sgAngptl3_SA off-target sites exhibited low (<0.5%) but statistically significant indel formation, including OT10_SA (Figure S2B). Off-target site 10 is located on chromosome 9 within *Gm19324*, a predicted gene with unknown functions. In contrast, none of the six successfully amplified potential off-target loci for sgAngptl3_SD showed increased A-to-G editing, and only two of the six exhibited very low (<0.04%) but significant indel formation above untreated controls (Figures S2C and S2D). Finally, to determine the potential hepatotoxicity of our LNPs, we analyzed serum alanine transaminase (ALT) at 6 and 48 h after LNP administration. Compared with untreated controls, mice treated

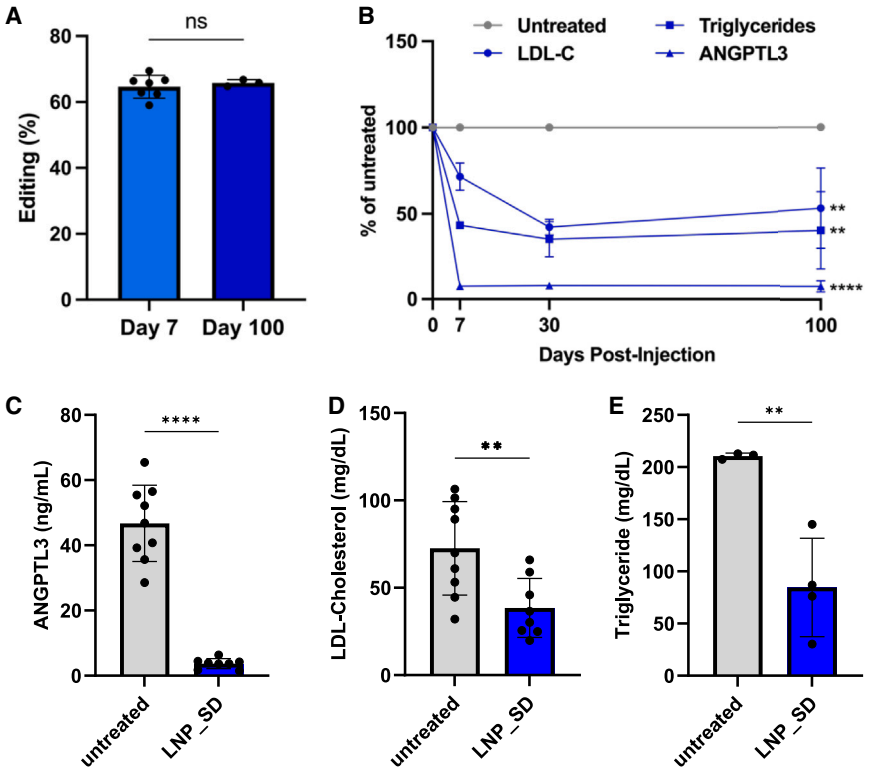

Figure 3. LNPs enable durable editing and serum reductions of fats in mice up to 100 days

(A) Total editing in mouse livers 7 and 100 days after administration of LNP_SD (n = 3–7). (B) Serum levels of ANGPTL3 (n = 4–11), LDL-C (n = 3–9), and TGs (n = 3–4) at days 7, 30, and 100 post injection, presented as percent of untreated controls. Statistics are relative to untreated controls for that measurement at day 100, as seen in (C–E). (C) Serum levels of ANGPTL3 (n = 8–9), (D) LDL-C (n = 8–9), and (E) TGs (n = 3-5) at day 100 after injection, presented as the raw values. Results displayed as mean ± standard deviations. Significance determined by unpaired Student's t test. $^{**}p < 0.01$, $^{****}p < 0.0001$.

with LNP_SA and LNP_SD demonstrated significantly elevated serum ALT at 6 h after administration (Figure 2G). After 48 h, mice treated with LNP_SA maintained high ALT levels, whereas no significant difference in ALT was observed between untreated controls and LNP_SD-treated mice (Figure 2H). However, as there was no statistically significant difference in ALT levels between LNP_SA and LNP_SD at 48 h, we cannot be fully confident that LNP_SA is more immunogenic.

Overall, our findings indicate that LNP_SD exhibits a favorable profile with lower indel rates, an elevated edit-to-indel ratio, diminished editing in the spleen, and fewer off-target editing events when compared with LNP_SA. Therefore, LNP_SD was selected as the formulation for subsequent analysis.

Angptl3 knockout reduces serum ANGPTL3, LDL-C, and TG levels up to 100 days

Sustained editing at the *Angptl3* locus is critical for demonstrating a potential one-and-done treatment for dyslipidemia-related diseases. Long-term therapeutic effects were analyzed up to 100 days after LNP administration, with serum analysis of ANGPTL3, LDL-C, and TG occurring at days 7, 30, and 100. Notably, no significant differences in editing levels were observed in the liver of mice administered LNP_SD at day 7 (64.6%) or day 100 (65.8%) (Figure 3A). Compared with untreated controls, mice injected with LNP_SD exhibited a 92.6% reduction in serum ANGPTL3 by day 7 (Figures 3B and S3A). Importantly, a significant decrease in serum ANGPTL3 was sustained at over 92% for the remainder of the study, aligning with the high editing levels at day 100 (Figures 3B, 3C, and S3A). Mice treated with LNP_SD exhibited statistically significant reductions in serum LDL-C of 28.5%, 57.7%, and 47% compared with untreated controls at days 7, 30, and 100, respectively (Figures 3B–3D and S3B). Finally, a durable reduction in TG levels was also observed. Compared with untreated controls, mice treated with LNP_SD exhibited a decrease in serum TG of 56.4%, 64.7%, and 59.8% at days 7, 30, and 100, respectively (Figures 3B–3E and S3C). Taken together, we demonstrate sustained editing with LNP_SD for up to 100 days with statistically significant reductions in serum ANGPTL3, LDL-C, and TG, signifying a potential therapy for CVD.

Angptl3 knockout maintains reduced lipid levels despite a high-fat, high-cholesterol diet challenge

Elevated blood levels of LDL-C and TGs in individuals susceptible to CVD frequently results from the consumption of a diet rich in cholesterol and fats. To determine whether our gene editing strategy maintains a therapeutic effect when challenged with a comparable diet, mice treated with LNP_SD were started on a high-fat high-cholesterol diet (HFHCD) 100 days post-treatment and continued for 13 weeks (91 days) (Figure 4A). The 13-week duration was chosen because previous work demonstrated that mice on an HFHCD for 13 weeks exhibit atherosclerosis and diet-induced obesity.[34] Editing levels in the liver remained high after HFHCD, at 56.1% (Figure 4B). Serum levels of ANGPTL3, LDL-C, and TGs were reduced by 88.9%, 44.7%, and 36.1%, respectively, compared with untreated mice also fed an HFHCD (Figures 4C–4E). Our results demonstrate that *Angptl3* knockout can durably reduce blood lipid levels even when challenged with an HFHCD.

LNPs enable efficient multiplex base editing at *Angptl3* and *Pcsk9*

CVD and other diseases originating in the liver may benefit from the ability to edit multiple disease-causing genes simultaneously or to

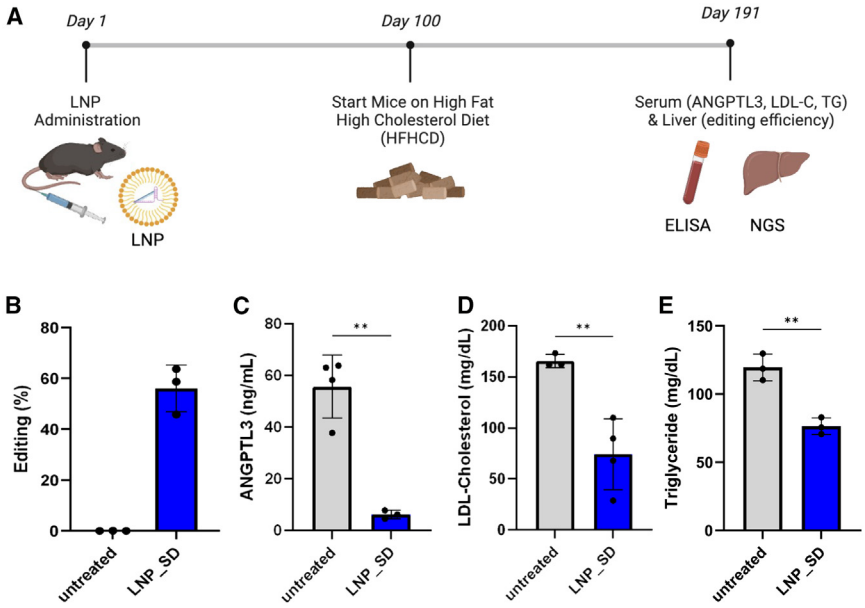

Figure 4. Therapeutic reductions in blood lipid levels are maintained after a HFHCD challenge

(A) Experimental timeline shows mice injected at day 1, started on a HFHCD diet at day 100, and euthanized at day 191, 13 weeks after initiation of HFHCD. Serum and liver samples were collected at day 191 for ELISAs and NGS, respectively. (B) Total editing in mouse livers 191 days after LNP administration (n = 3). (C) Serum levels of ANGPTL3 (n = 3), (D) LDL-C (n = 3–4), and (E) TGs (n = 3). Results displayed as mean ± standard deviation. Significance determined by unpaired Student's t test. $^{**}p < 0.01$.

correct a disease phenotype while selectively expanding gene-edited hepatocytes.[35,36] Building on the success of our LNP base editing system in achieving high efficiency single-target editing, we aimed to provide a proof of concept for multiplex *in vivo* base editing at clinically relevant targets.

Pcsk9 represents another target gene to treat CVD that was previously edited with ABEs in mice and non-human primates.[3,4] Recent studies suggest that pharmacological inhibition of ANGPTL3 and PCSK9 simultaneously could have additive or even synergistic effects.[37,38] As a preliminary investigation into the feasibility of multiplex *in vivo* base editing with our LNPs, *Angptl3* and *Pcsk9* were targeted concurrently. LNPs were formulated with a 1:1 ratio of total sgRNA to ABE8e mRNA and administered at a single dose of 3 mg/kg. For multiplex base editing, the ratio of total sgRNA:ABE8e mRNA remained 1:1. However, the total sgRNA was composed of a 1:1 ratio of *Angptl3* sgRNA to *Pcsk9* sgRNA. This strategy was chosen to ensure optimal codelivery of both the sgRNAs and mRNA into the liver, where each sgRNA retains an equal amount of ABE8e mRNA for eventual formation of catalytically active ribonucleoprotein complexes.[39] When targeting *Angptl3* alone, we observed robust editing of 66.8% and 64.8% for sgAngptl3_SA and sgAngptl3_SD, respectively, which was consistent with earlier data. When targeting *Pcsk9* alone, we also achieved high editing frequencies of 66.7% (Figures 5A and 5B). Notably, multiplex editing resulted in no significant changes in the editing efficiency at *Pcsk9* (65.9% and 67.7% when multiplexed with sgAngptl3_SA and sgAngptl3_SD, respectively), while a minimal decrease in editing was observed at *Angptl3* (59.9% and 52.1% with sgAngptl3_SA and sgAngptl3_SD, respectively). This proof-of-concept multiplex study suggests that co-inhibition of ANGPTL3 and PCSK9 is achievable with our LNP delivery system, demonstrating the potential for targeting multiple genes involved in CVD or other disease processes where multiplexing is necessary.

Concurrent genome editing at multiple loci may increase the likelihood of translocations when targeted loci are on different chromosomes, or large deletions or inversions when targeted loci are on the same chromosome. Prior work has shown that translocations yielded from multiplex cytidine base editing was substantially reduced relative to Cas9 nuclease and were not detected after multiplex adenine base editing.[40,41] To evaluate whether multiplex adenine base editing of *Angptl3* and *Pcsk9* induces unintended genomic alterations, we conducted PCR assays to detect potential deletions or inversions, as both genes are located on mouse chromosome 4. While inversions and large deletions were detected in all positive control samples electroporated with Cas9 mRNA and the same guide RNAs, PCR analysis of three mice treated with ABE8e mRNA and sgAngptl3_SD and sgPcsk9 guide RNAs revealed no evidence of inversions and only one mouse where PCR amplification of a large deletion was observed, albeit more faintly than for the nuclease-treated control (Figures S4A–S4D). These findings suggest that our *in vivo* multiplex editing strategy does not lead to frequent undesired outcomes like inversions or large deletions.

DISCUSSION

Current treatment recommendations for CVD include lifestyle changes and chronic medication. However, these options suffer from poor patient adherence, leading to adverse patient outcomes. In contrast, gene therapy could provide a one-and-done treatment option by targeting key genes involved in lipid metabolism and permanently lowering blood levels of LDL-C and TGs, which are key contributors to CVD. In our study, we found that ABEs packaged in a liver-targeting LNP were effective in knocking out *Angptl3* in the liver and leading to durable reductions in serum ANGPTL3, LDL-C, and TGs for up to 100 days.

In vivo gene therapy is complicated by the difficulty of delivering gene editing apparatus, such as BE mRNA and sgRNAs, to a targeted organ and without degrading the RNA in the process. While the U.S. Food

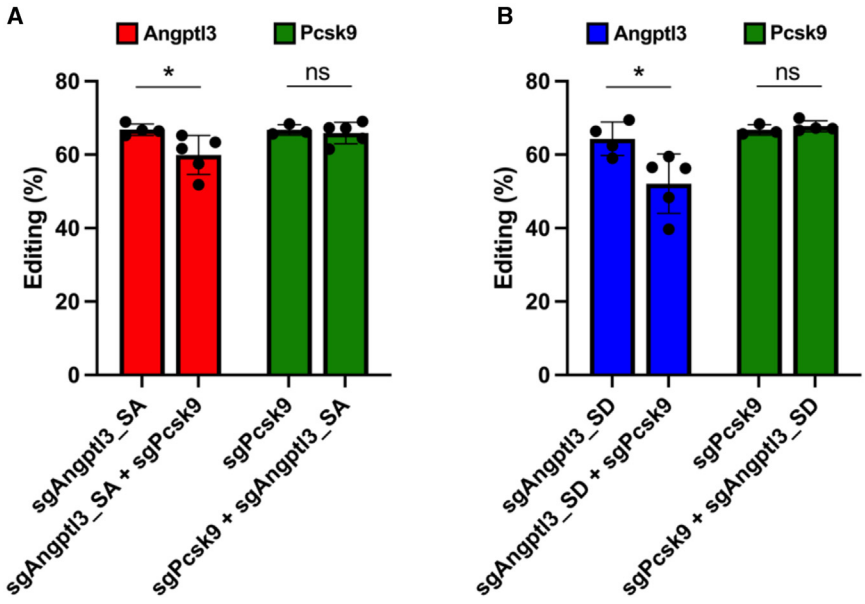

Figure 5. Efficient *in vivo* multiplex base editing at Angptl3 and Pcsk9

(A) Total editing in mouse livers 7 days after administration of LNPs packaged with ABE8e mRNA and either sgAngptl3_SA, sgPcsk9, or sgAngptl3_SA and sgPcsk9. Editing levels at the *Angptl3* splice acceptor site (red) and the *Pcsk9* locus (green). (B) Total editing in mouse livers 7 days after administration of LNPs packaged with ABE8e mRNA and either sgAngptl3_SD, sgPcsk9, or sgAngptl3_SD and sgPcsk9. Editing levels at the *Angptl3* splice donor site (blue) and the *Pcsk9* locus (green). Results displayed as mean ± standard deviation. Significance determined by unpaired Student's t test. $^{*}p < 0.05$.

and Drug Administration has recently approved gene editing products for the treatment of sickle cell disease and others, clinical trials using LNPs containing genome editing tools are ongoing for the treatment of hereditary transthyretin amyloidosis and hereditary angioedema.[42] Using a newly synthesized liver-targeting lipid, L88, our LNP formulations consistently led to base editing rates of approximately 60% in the mouse liver at two target sites, which is comparable with the highest reported standards in the literature. ANGPTL3 is primarily expressed by liver hepatocytes, which make up roughly 60%–70% of cells in the liver.[4,28,43] Given that our editing resulted in a reduction in serum ANGPTL3 by approximately 92%, our results suggest we achieved biallelic editing in nearly all hepatocytes, highlighting the efficiency of our system. Importantly, we showed that high editing rates in the liver did not compromise tissue tropism. While LNPs formulated with L88 achieved approximately 60% editing in the liver, editing was observed at lower than 2% in the spleen and was undetectable in all other tested organs. LNP uptake by the spleen has been observed in other studies and is to be expected in small amounts.[4]

In a previous report, we described the use of 306-O12B LNPs to deliver Cas9 mRNA and sgRNAs to the mouse liver to knockout *Angptl3*.[15] We achieved approximately 38% editing in the liver at day 7 and reductions in LDL-C and TG for up to 100 days. In the current study, LNPs formulated with a newly synthesized lipid, L88, and packaged with ABE8e mRNA and sgRNAs, demonstrated substantially higher editing rates. As we did not test the use of Cas9 mRNA in our new LNP formulations, or base editing with 306-O12B LNPs, it remains unclear whether the improved editing rates are due to the use of new lipids, superiority of BEs over Cas9 nuclease, or a mix of both. Further work is needed to dissect this question and is currently underway. One benefit of using BEs over Cas9 is its ability to generate precise nucleotide conversions without generating DNA DSBs, which have been shown to result in complex deletions, translocations, and chromosomal rearrangements. Our optimized LNP formulation, LNP_SD, exhibited 64.6% base editing at our target site, while indel rates remained below 1.5%. Compared with our Cas9 approach, this editing strategy allowed for more efficient editing while reducing indel formation by more than 95%. Overall, we achieved an edit-to-indel ratio of 44.2.

As our therapeutic approach is intended as a one-and-done treatment, it was imperative to show the ability of LNP_SD to maintain high editing levels and durably reduce serum LDL-C and TG. We found no change in editing frequencies between 7 and 100 days after treatment, highlighting the enduring nature of the edits. Moreover, durable reductions in LDL-C and TGs up to 100 days after treatment suggest a lasting effect of this potential therapy on inhibiting blood lipid levels. As dyslipidemia in CVD patients is often due to diets rich in cholesterol and fats, we assessed the long-term effects of our therapeutic approach when challenged with an HFHCD for 13 weeks, a regimen known to induce atherosclerosis and diet-induced obesity in mice.[34] We found that, compared with untreated mice on an HFHCD, mice treated with LNP_SD maintained lower levels of LDL-C and TG when on an HFHCD. Additionally, serum levels of LDL-C and TG were comparable with those observed before the initiation of an HFHCD.

Ensuring the safety and efficacy of our approach is paramount for advancing our genome editing strategy toward clinical applications. Comprehensive safety profiling is crucial, including experimental off-target analysis in the human genomic context. Using Cas-OFFinder, we identified 20 predicted off-target sites in the mouse genome with 3 mismatches to the protospacer of sgAngptl3_SA compared with just 7 sites with 3 mismatches to sgAngptl3_SD. Recent studies have shown that off-target effects with ABEs decrease significantly with three or more mismatches, suggesting that both of our *Angptl3*-targeting sgRNAs have a favorable specificity for on-target editing.[44] Of the amplifiable off-target loci, 1 of the 15 sgAngptl3_SA sites and none of the 6 sgAngptl3_SD sites exhibited a significant increase in A-to-G editing. We found a 5.29% increase

in A-to-G editing at OT10_SA, a region of chromosome 9 located within *Gm19324*, a predicted gene with unknown functions. While assessing indel formation at each off-target loci, we found that two of the 15 sgAngptl3_SA sites, including OT10_SA, and 2 of the 6 sgAngptl3_SD sites demonstrated low (<0.5% for sgAngptl3_SA and <0.04% for sgAngptl3_SD) but significant editing. However, while the exon 6 splice acceptor and splice donor sites are targetable with ABEs using the same PAM positioning at the human *ANGPTL3* locus, the exact sgRNA sequence differs by two and four sequences from the mouse sgRNA sequences, respectively. This means that potential off-target sites may differ between mouse and human sgRNAs and will require further investigation, including an assessment of genotoxic effects in the human genome.[40] Another important aspect of safety profiling is liver toxicity. Our study measured ALT levels at 6 and 48 h after infusion and found a return to baseline ALT levels for LNP_SD at 48 h. This suggests that LNP_SD does not cause prolonged liver toxicity. However, further long-term studies are necessary to confirm the absence of liver toxicity and the overall safety of our approach. While our results provide a strong foundation for the specificity of our base editing approach and show minimal indel formation at both on-target and off-target sites, particularly when using sgAngptl3_SD, these additional investigations will provide a more comprehensive understanding of the long-term effects and safety of our LNP formulations.

We also demonstrated efficient *in vivo* multiplex base editing by simultaneously targeting *Angptl3* and *Pcsk9*, with no detectable evidence of inversions and only a single mouse exhibiting a large deletion. Concurrent inhibition of ANGPTL3 and PCSK9 represents a promising strategy to further reduce blood lipid levels. While our current study focuses on demonstrating the feasibility and efficiency of this multiplex base editing approach, assessing LDL-C and TG levels following the *Angptl3-Pcsk9* double knockout will be vital in future investigations to fully evaluate the therapeutic potential of this strategy. Importantly, this multiplex approach can be applied to other liver-related diseases with multiple disease-causing mutations. Multiplex editing could also potentially be used to introduce a variant that can be subsequently selected for, permitting expansion of edited cells even when low dose-low efficiency editing is applied.[35,36]

Overall, this study shows promise in developing an efficient *in vivo* base editing strategy for a one-and-done treatment for CVD patients.

MATERIALS AND METHODS

Study design

The overall study was designed to (1) identify newly synthesized liver-targeting LNPs with the highest transfection and editing efficiency and (2) evaluate the long-term editing efficiency of our optimized LNP formulations and assess their capacity to maintain reductions in serum LDL-C and TG.

sgRNA design

Splice site targeting sgRNAs were designed with SpliceR (http://z.umn.edu/spliceR), as previously described.[26] Candidate sgRNAs were selected based on their predicted editing efficiency and the conservation of PAM sites within the human *ANGPTL3* gene, thereby ensuring their relevance for potential clinical application in human patients (Table 1). The 100-nt sgRNAs bearing an exon 6 splice acceptor 20-mer (sgAngptl3_SA; 5′-TCTTTAGGAGAATTTTGG TT-3′) or exon 6 splice donor 20-mer (sgAngptl3_SD; 5′-GAGA TACCTGAGTAACTTTC-3′) were chemically synthesized by Synthego. The modified synthetic sgRNAs contained 2′-O-methyl analogs on the first and last three bases and 3′ phosphorothioate internucleotide linkages between the first three and last two bases. A sgRNA targeting the exon 1 splice donor site of *Pcsk9* (sgPcsk9; 5′-CCCA TACCTTGGAGCAACGG-3′) was synthesized, as above.

Lipid synthesis

L88 was synthesized through Michael addition reactions. 3,3′-Diamino-N-methyldipropylamine (amine head 306) and an acrylate tail 88 (5 eq.) were mixed in a Teflon-lined glass screw-top vial and heated at 70°C for 48 h.[32] For synthesis of L10, a 3,3′-diamino-N-methyldipropylamine (amine head 306) and an acrylate tail O12B (3.2 eq.) were mixed in a Teflon-lined glass screw-top vial and heated at 70°C for 48 h. For both lipids, the crude products were then purified by a Teledyne Isco Chromatography system using methanol/DCM as mobile phase. The fractions containing the desired products, which were checked by TLC and electrospray ionization mass spectrometry, were pooled and concentrated to afford L88 or L10. Lipid 306-O12B was synthesized as previously described.[15]

mRNA synthesis

Addgene plasmid ID: 221654 was PCR amplified using this forward primer that corrects the inactive T7 promoter on the plasmid, preventing round-the-plasmid transcription: 5′-TCGAGCTCGGTACC TAATACGACTCACTATAAGG-3′ and with this reverse primer that adds a 120nt polyA tail: 5′-TTTTTTTTTTTTTTTTTTTTTT TTTTTTTTTTTTTTTTTTTTTTTTTTTTTTTTTTTTTTTTTTTTTTT TTTTTTTTTTTTTTTTTTTTTTTTTTTTTTTTTTTTTTTTTTTTTTT TTTTTTTTTTCTTCCTACTCAGGCTTTATTCAAAGACCA-3′. PCR consisted of a 2-min denaturation at 98°C followed by 30 cycles of (15 s denaturation at 98°C, 20 s annealing at 71.4°C, and 1.5 min extension at 72°C), followed by a final extension at 72°C for an additional 2 min. Amplified DNA was purified using a Qiagen PCR clean-up kit and quantified by nanodrop. To transcribe RNA, we used the NEB T7 HiScribe kit (Cat. No. E2040L). Transcription was conducted according to manufacturer instructions, using full substitution of UTP for N1-methylpseudouridine-5′-triphosphate (Trilink Cat. No. *N*-1081) and with 100 mM CleanCap AG (Trilink Cat. No. *N*-7113) and with 1 μg of DNA per 40 μL transcription reaction. Transcription was conducted for 2 h at 37°C. Following transcription, mRNA was purified using a lithium chloride precipitation. 7.5M lithium chloride (Thermo Fisher Scientific AM9480) was diluted to a final concentration of 2.5 M directly in the transcription solution. The solution was chilled at −20°C for 30 min. Precipitated mRNA was pelleted by centrifuging samples at 12,000 × *g* on a benchtop microcentrifuge for 15 min. The supernatant was discarded and the pellet was washed with chilled 70% ethanol using a slightly larger volume

Table 1. Protospacer sequence and PAM for candidate sgRNAs in both mice and human

sgRNA	Mouse protospacer/PAM (5′ to 3′)	Human protospacer/PAM (5′ to 3′)
sgAngptl3_SA	TCTTT**A**GGAGAATTTTGGTT/GGG	TTTTC**A**GGAGAATTTTGGTT/GGG
sgAngptl3_SD	GAGAT**A**CCTGAGTAACTTTC/TGG	AAGAT**A**CCTGAATAACCCTC/TGG

Target nucleotides are in bold/underline.

than the original supernatant. After inversion and vortexing, mRNA was pelleted again by a second centrifugation at 12,000×*g* for 15 min. Supernatant was discarded and residual ethanol was pipetted away and dried by placing open tubes in a biosafety cabinet to dry for 2 min. All mRNAs were normalized at a concentration of 1.6 or 2 μg of mRNA per microliter and stored at −80°C. Yield was approximately 80–120 μg of mRNA per 40 μL transcription reaction.

Formulation of LNPs

LNPs were synthesized using previously established protocols with modifications.[15] LNPs were prepared using a NanoAssemblr microfluidic system (Precision Nanosystems) at a flow ratio of 3:1 (aqueous:organic) and flow rate of 12 mL/min. For *in vivo* luciferase mRNA delivery, blank LNPs were prepared. The organic phase was prepared by mixing lipid (L88, L10, or lipid 306-O12B), cholesterol, 1,2-dioleoyl-sn-glycero-3-phosphocholine (DOPC), and 1,2-dimyristoyl-rac-glycero-3-methoxypolyethylene glycol-2000 (DMG-PEG 2000) at the defined weight ratio (16:4:2:1). The aqueous phase was 25 mM sodium acetate (pH 5.4). The resulting LNPs were then dialyzed in the Slide-A-Lyzer MINI Dialysis Device (Thermo Fisher Scientific) with a molecular weight cut off (MWCO) of 3.5 KDa in PBS at 4°C for 4 h. Blank LNPS were mixed with luciferase mRNA at a weight ratio of 10:1 (active lipid:mRNA) in aqueous solution. For base editing experiments, the organic phase was prepared by mixing lipid (L88 or L10), cholesterol, DOPC, and DMG-PEG 2000 at a molar ratio of 45.8:41.6:11.0:1.6, respectively, and dissolving in pure ethanol at a concentration of 15 mg/mL. The aqueous phase was prepared by dissolving total sgRNA (Synthego) and ABE8e mRNA at a ratio of 1:1 in 25 mM sodium acetate at a concentration of 10.46 mg/mL of total RNA. For multiplex base editing, the ratio of total sgRNA:ABE8e mRNA remained 1:1. However, the total sgRNA was composed of a 1:1 ratio of *Angptl3* sgRNA to *Pcsk9* sgRNA. The resulting LNPs were then dialyzed in the Slide-A-Lyzer MINI Dialysis Device (Thermo Fisher Scientific) with an MWCO of 3.5 KDa in PBS at 4°C for 4 h. Size and zeta potential of dialyzed LNPs were measured with dynamic light scattering (DLS) using a Malvern ZetaPALS DLS machine (Brookhaven Instruments).

Animal studies

All animal experiments were approved by Tufts University Institutional Animal Care and Use Committee and performed in accordance with the National Institutes of Health guidelines for the care and use of experimental animals. All mice were randomly assigned to various experimental and control groups. For *in vivo* luciferase assay, LNPs containing 5 μg luciferase mRNA and 50 μg active lipid were administered via IV tail vein injection to 4- to 6-week-old BALB/c mice (Charles River Laboratories). Six hours after the injection, 100 μL of D-luciferin (15 mg/mL) was intraperitoneally injected into the mice. After 10 min, the mice, anesthetized under isoflurane, were imaged using the In Vivo Imaging System and processed with Living Image analysis software (Perkin Elmer). For base editing experiments, LNPs were administered to 6- to 8-week-old female C57BL/6J mice (Charles River Laboratories) via IV tail vein injection at a total RNA dose of 3 mg/kg (unless otherwise stated).

NGS analysis

To assess editing rates, DNA was extracted from organs using a Qiagen DNEasy Blood and Tissue kit. For liver analysis, DNA was extracted from the median and left lateral lobe. Genomic DNA was amplified by PCR using primers specific to the target genomic sites—designed with Primer3 v.4.1.0 (https://primer3.ut.ee/)—containing adapters for Illumina sequencing (Table 2). The PCR reaction contained 0.4 μM of each primer, 1× Q5 High-Fidelity Master Mix (New England Biolabs) or 1× Phusion U Multiplex PCR Master Mix (Thermo Fisher Scientific), 100 ng genomic DNA, and water to a final volume of 25 μL. The following PCR program was used: step 1, 95°C for 2 min; step 2, 98°C for 10 s; step 3, annealing for 30 s (annealing temperatures for respective primer sets are detailed in Table 2); step 4, 72°C for 2 min; step 5, repeat steps 2–4 for a total of 30 cycles; step 6, 72°C for 2 min; and step 7, 4°C. After Illumina barcoding, PCR products were purified by electrophoresis with a 2% agarose gel using a Monarch DNA Gel Extraction Kit (New England Biolabs) or QIAquick Gel Extraction Kit (Qiagen), eluting with 30 μL H_2O. DNA concentration was quantified using a Quibit dsDNA High Sensitivity Assay Kit (Thermo Fisher Scientific) and by qPCR using the KAPA Library Quantification Kit (Roche) before being sequenced on an Illumina MiSeq instrument (single-end read, 250–300 cycles) according to the manufacturer's protocols. Alignment of fastq files and quantification of editing frequency were performed using CRISPResso2 in batch mode with a window width of 24 nucleotides.[45] Total editing percentage was quantified by summing the A-to-G, A-to-C, and A-to-T edits at the target nucleotide.

Serum ELISAs

Blood samples were taken at various timepoints either via sublaminar cheek blood draw or cardiac punctures. Blood was allowed to clot for 2 h at room temperature and then was centrifuged at 5,400 rpm for 10 min. ELISAs were conducted to measure serum levels of ANGPTL3 (R&D Systems), LDL-C (Crystal Chemical), TGs (Cayman Chemical), and ALT (G-Biosciences). Absorbance levels

Table 2. PCR primers for target site amplification

Site	Forward primer (5′ to 3′)	Reverse primer (5′ to 3′)	Annealing temperature (°C)
Angptl3 Exon 6 SA	**ACACTCTTTCCCTACACGACGCT CTTCCGATCTNNNN**ACGTGTCAG TCAGGTCCTG	**TGGAGTTCAGACG TGTGCTCTTCCGATCT**TTTCTGGA CAGTAGAGCTGTC	60
Angptl3 Exon 6 SD	**ACACTCTTTCCCTACACGACGCT CTTCCGATCTNNNN**ACATGTGGC TGAGATTGCTG	**TGGAGTTCAGAC GTGTGCTCTTCCGATCT**CACCAC CAGCCACCTAAAAA	62
Pcsk9 Exon 1 SD	**ACACTCTTTCCCTA CACGACGCTCTTCCGATCTNNNN** GCTGCTGTTGCTGCTACTGT	**TGGA GTTCAGACGTGTGCTCTTCCGATC TCAAGGTGCAGCTGAGCACTA**	60

Adapters for Illumina sequencing are in bold.

were measured using Thermo Fisher Scientific Varioskan LUX microplate reader.

Off-target prediction and analysis

The Cas-OFFinder on-line search tool (available at http://www.rgenome.net/cas-offinder/) was used to search the mouse genome (GRCm38/mm10) for potential *Streptococcus pyogenes* Cas9 off-target sites (PAM = 5′-NGG-3′) using the unique, target-specific portion of the sgRNAs used in this study (sgAngptl3_SA: 5′-TCTTTAGGAGAATTTTGGTT -3′; sgAngptl3_SD: 5′- GAGATA CCTGAGTAACTTTC -3′) as a query sequence while allowing for up to three mismatched base pairs between the sgRNA and candidate target sites.[46] DNA was extracted from the median lobe of livers in untreated or treated mice seven days after LNP administration. Genomic DNA was amplified by PCR using primers specific to the off-target genomic sites and sequenced on an Illumina MiSeq instrument as described above in Methods: NGS analysis (Table S4).

Inversions and deletions analyses

For a Cas9 nuclease control, sgAngptl3_SD and sgPcsk9 were co-delivered to N2a cells with Cas9 mRNA (TriLink, Cat. No. L-8106) via electroporation using the Lonza 4D Nucleofector with SF solution and code DS-137. We electroporated 1,000,000 cells per replicate in 20 μL volumes with 1.5 μL (2 μg) of mRNA and 0.5 μL of each 100 μM guide RNA, or water for a mock negative control. DNA was extracted after 72 h as previously described.[47] For multiplex editing conditions, LNPs were formulated with ABE8e mRNA and sgAngptl3_SD:sgPcsk9 at a 1:1 ratio, as described above. We amplified 100 ng of genomic DNA from electroporated cells and mouse livers using a matrix of PCR primers binding to each side of both editing loci (Table 2; Figure S4A). The PCR reactions contained 0.3 μM of each primer, 1× KAPA HiFi HotStart Mix (Roche/Kapa biosystems), 100 ng genomic DNA, and water to a final volume of 25 μL. The following PCR program was used: step 1, 98°C for 2 min; step 2, 95°C for 15 s; step 3, 63°C for 15 s; step 4, 72°C for 15 s; step 5, repeat steps 2–4 for a total of 45 cycles; step 6, 72°C for 2 min; and step 7, 4°C. A high cycle number is necessary due to low proportion of template genomic DNA containing these undesired editing outcomes; a higher annealing temperature is used to reduce non-specific amplification that can occur due to the high cycle number. DNA amplicons were resolved by capillary electrophoresis on a QIAxcel Connect System (Qiagen) using a DNA High Resolution kit according to the manufacturer's instructions.

Statistics

Graphs were produced using GraphPad Prism 10.0.0 Software and statistical analysis was determined. Statistical analysis in experiments containing two groups was performed using a two-tailed Student's t test, whereas analysis in experiments with more than two groups was performed by one-way ANOVA with Tukey-Kramer test to compare individual means. $*p < 0.05$ was considered statistically significant. $**p < 0.01$, $***p < 0.001$ $****p < 0.0001$.

DATA AVAILABILITY

Original data can be accessed upon request.

ACKNOWLEDGMENTS

J.K. is supported by the National Science Foundation (NSF) Graduate Research Fellowships Program (GRFP) Grant DGE-184274. H.B. acknowledges support by NIH Grant No. 5T32 GM008448-27. Q.X. acknowledges support by NIH Grant No. UG3 TR002636-01. G.A.N. acknowledges support by NIH Grant No. R00 HL163805. J.N.W. acknowledges support by NIH Grant No. T32 GM148383. This article is subject to HHMI's Open Access to Publications policy. HHMI lab heads have previously granted a nonexclusive CC BY 4.0 license to the public and a sublicensable license to HHMI in their research articles. Pursuant to those licenses, the author-accepted manuscript of this article can be made freely available under a CC BY 4.0 license immediately upon publication.

AUTHOR CONTRIBUTIONS

J.K., H.B., G.A.N., Y.L., D.R.L., and Q.X. designed the experiments. J.K. and H.B. performed the majority of experiments and analyzed all data. J.N.W. and G.A.N. produced ABE8e mRNA and performed DNA sequencing. J.N.W. performed PCR for off-target assessment and PCR and capillary electrophoresis for inversion/deletion analysis. D.W. assisted with organ harvesting, maintaining diets, and running ELISAs. C.F. generated lipids. J.K., H.B., and Q.X. wrote and edited the manuscript. G.A.N. edited the manuscript.

DECLARATION OF INTERESTS

The authors declare competing financial interests: D.R.L. is a consultant and/or equity owner for Prime Medicine, Beam Therapeutics, Pairwise Plants, Chroma Medicine, and Nvelop Therapeutics, companies that use or deliver genome editing or epigenome engineering agents.

SUPPLEMENTAL INFORMATION

Supplemental information can be found online at https://doi.org/10.1016/j.omtn.2025.102486.

REFERENCES

1. Adhikary, D., Barman, S., Ranjan, R., and Stone, H. (2022). A Systematic Review of Major Cardiovascular Risk Factors: A Growing Global Health Concern. Cureus *14*, e30119. https://doi.org/10.7759/cureus.30119.
2. Virani, S.S., Alonso, A., Benjamin, E.J., Bittencourt, M.S., Callaway, C.W., Carson, A.P., Chamberlain, A.M., Chang, A.R., Cheng, S., Delling, F.N., et al. (2020). Heart Disease and Stroke Statistics-2020 Update: A Report From the American Heart Association. Circulation *141*, e139–e596. https://doi.org/10.1161/CIR.0000000000000757.
3. Musunuru, K., Chadwick, A.C., Mizoguchi, T., Garcia, S.P., DeNizio, J.E., Reiss, C.W., Wang, K., Iyer, S., Dutta, C., Clendaniel, V., et al. (2021). In vivo CRISPR base editing of PCSK9 durably lowers cholesterol in primates. Nature *593*, 429–434. https://doi.org/10.1038/s41586-021-03534-y.
4. Rothgangl, T., Dennis, M.K., Lin, P.J.C., Oka, R., Witzigmann, D., Villiger, L., Qi, W., Hruzova, M., Kissling, L., Lenggenhager, D., et al. (2021). In vivo adenine base editing of PCSK9 in macaques reduces LDL cholesterol levels. Nat. Biotechnol. *39*, 949–957. https://doi.org/10.1038/s41587-021-00933-4.
5. Koishi, R., Ando, Y., Ono, M., Shimamura, M., Yasumo, H., Fujiwara, T., Horikoshi, H., and Furukawa, H. (2002). Angptl3 regulates lipid metabolism in mice. Nat. Genet. *30*, 151–157. https://doi.org/10.1038/ng814.
6. Romeo, S., Yin, W., Kozlitina, J., Pennacchio, L.A., Boerwinkle, E., Hobbs, H.H., and Cohen, J.C. (2009). Rare loss-of-function mutations in ANGPTL family members contribute to plasma triglyceride levels in humans. J. Clin. Investig. *119*, 70–79. https://doi.org/10.1172/JCI37118.
7. Tarugi, P., Bertolini, S., and Calandra, S. (2019). Angiopoietin-like protein 3 (ANGPTL3) deficiency and familial combined hypolipidemia. J. Biomed. Res. *33*, 73–81. https://doi.org/10.7555/JBR.32.20170114.
8. Stitziel, N.O., Khera, A.V., Wang, X., Bierhals, A.J., Vourakis, A.C., Sperry, A.E., Natarajan, P., Klarin, D., Emdin, C.A., Zekavat, S.M., et al. (2017). ANGPTL3 Deficiency and Protection Against Coronary Artery Disease. J. Am. Coll. Cardiol. *69*, 2054–2063. https://doi.org/10.1016/j.jacc.2017.02.030.
9. Wang, J., Zheng, W., Zheng, S., Yuan, Y., Wen, W., Cui, W., Xue, L., Sun, X., Shang, H., Zhang, H., et al. (2023). Targeting ANGPTL3 by GalNAc-conjugated siRNA ANGsiR10 lowers blood lipids with long-lasting and potent efficacy in mice and monkeys. Mol. Ther. Nucleic Acids *31*, 68–77. https://doi.org/10.1016/j.omtn.2022.11.023.
10. Graham, M.J., Lee, R.G., Brandt, T.A., Tai, L.J., Fu, W., Peralta, R., Yu, R., Hurh, E., Paz, E., McEvoy, B.W., et al. (2017). Cardiovascular and Metabolic Effects of ANGPTL3 Antisense Oligonucleotides. N. Engl. J. Med. *377*, 222–232. https://doi.org/10.1056/NEJMoa1701329.
11. Raal, F.J., Rosenson, R.S., Reeskamp, L.F., Hovingh, G.K., Kastelein, J.J.P., Rubba, P., Ali, S., Banerjee, P., Chan, K.C., Gipe, D.A., et al. (2020). Evinacumab for Homozygous Familial Hypercholesterolemia. N. Engl. J. Med. *383*, 711–720. https://doi.org/10.1056/NEJMoa2004215.
12. Dewey, F.E., Gusarova, V., Dunbar, R.L., O'Dushlaine, C., Schurmann, C., Gottesman, O., McCarthy, S., Van Hout, C.V., Bruse, S., Dansky, H.M., et al. (2017). Genetic and Pharmacologic Inactivation of ANGPTL3 and Cardiovascular Disease. N. Engl. J. Med. *377*, 211–221. https://doi.org/10.1056/NEJMoa1612790.
13. Bloomer, H., Khirallah, J., Li, Y., and Xu, Q. (2022). CRISPR/Cas9 ribonucleoprotein-mediated genome and epigenome editing in mammalian cells. Adv. Drug Deliv. Rev. *181*, 114087. https://doi.org/10.1016/j.addr.2021.114087.
14. Shivram, H., Cress, B.F., Knott, G.J., and Doudna, J.A. (2021). Controlling and enhancing CRISPR systems. Nat. Chem. Biol. *17*, 10–19. https://doi.org/10.1038/s41589-020-00700-7.
15. Qiu, M., Glass, Z., Chen, J., Haas, M., Jin, X., Zhao, X., Rui, X., Ye, Z., Li, Y., Zhang, F., and Xu, Q. (2021). Lipid nanoparticle-mediated codelivery of Cas9 mRNA and single-guide RNA achieves liver-specific in vivo genome editing of Angptl3. Proc. Natl. Acad. Sci. USA *118*, e2020401118. https://doi.org/10.1073/pnas.2020401118.
16. Kosicki, M., Tomberg, K., and Bradley, A. (2018). Repair of double-strand breaks induced by CRISPR-Cas9 leads to large deletions and complex rearrangements. Nat. Biotechnol. *36*, 765–771. https://doi.org/10.1038/nbt.4192.
17. Shin, H.Y., Wang, C., Lee, H.K., Yoo, K.H., Zeng, X., Kuhns, T., Yang, C.M., Mohr, T., Liu, C., and Hennighausen, L. (2017). CRISPR/Cas9 targeting events cause complex deletions and insertions at 17 sites in the mouse genome. Nat. Commun. *8*, 15464. https://doi.org/10.1038/ncomms15464.
18. Zhang, L., Jia, R., Palange, N.J., Satheka, A.C., Togo, J., An, Y., Humphrey, M., Ban, L., Ji, Y., Jin, H., et al. (2015). Large genomic fragment deletions and insertions in mouse using CRISPR/Cas9. PLoS One *10*, e0120396. https://doi.org/10.1371/journal.pone.0120396.
19. Conti, A., and Di Micco, R. (2018). p53 activation: a checkpoint for precision genome editing? Genome Med. *10*, 66. https://doi.org/10.1186/s13073-018-0578-6.
20. Haapaniemi, E., Botla, S., Persson, J., Schmierer, B., and Taipale, J. (2018). CRISPR-Cas9 genome editing induces a p53-mediated DNA damage response. Nat. Med. *24*, 927–930. https://doi.org/10.1038/s41591-018-0049-z.
21. Geisinger, J.M., and Stearns, T. (2020). CRISPR/Cas9 treatment causes extended TP53-dependent cell cycle arrest in human cells. Nucleic Acids Res. *48*, 9067–9081. https://doi.org/10.1093/nar/gkaa603.
22. van den Berg, J., G Manjón, A., Kielbassa, K., Feringa, F.M., Freire, R., and Medema, R.H. (2018). A limited number of double-strand DNA breaks is sufficient to delay cell cycle progression. Nucleic Acids Res. *46*, 10132–10144. https://doi.org/10.1093/nar/gky786.
23. Gaudelli, N.M., Komor, A.C., Rees, H.A., Packer, M.S., Badran, A.H., Bryson, D.I., and Liu, D.R. (2017). Programmable base editing of A*T to G*C in genomic DNA without DNA cleavage. Nature *551*, 464–471. https://doi.org/10.1038/nature24644.
24. Komor, A.C., Kim, Y.B., Packer, M.S., Zuris, J.A., and Liu, D.R. (2016). Programmable editing of a target base in genomic DNA without double-stranded DNA cleavage. Nature *533*, 420–424. https://doi.org/10.1038/nature17946.
25. Rees, H.A., and Liu, D.R. (2018). Base editing: precision chemistry on the genome and transcriptome of living cells. Nat. Rev. Genet. *19*, 770–788. https://doi.org/10.1038/s41576-018-0059-1.
26. Kluesner, M.G., Lahr, W.S., Lonetree, C.L., Smeester, B.A., Qiu, X., Slipek, N.J., Claudio Vázquez, P.N., Pitzen, S.P., Pomeroy, E.J., Vignes, M.J., et al. (2021). CRISPR-Cas9 cytidine and adenosine base editing of splice-sites mediates highly-efficient disruption of proteins in primary and immortalized cells. Nat. Commun. *12*, 2437. https://doi.org/10.1038/s41467-021-22009-2.
27. Davis, J.R., Wang, X., Witte, I.P., Huang, T.P., Levy, J.M., Raguram, A., Banskota, S., Seidah, N.G., Musunuru, K., and Liu, D.R. (2022). Efficient in vivo base editing via single adeno-associated viruses with size-optimized genomes encoding compact adenine base editors. Nat. Biomed. Eng. *6*, 1272–1283. https://doi.org/10.1038/s41551-022-00911-4.
28. Zuo, Y., Zhang, C., Zhou, Y., Li, H., Xiao, W., Herzog, R.W., Xu, J., Zhang, J., Chen, Y.E., and Han, R. (2023). Liver-specific in vivo base editing of Angptl3 via AAV delivery efficiently lowers blood lipid levels in mice. Cell Biosci. *13*, 109. https://doi.org/10.1186/s13578-023-01036-0.
29. Taha, E.A., Lee, J., and Hotta, A. (2022). Delivery of CRISPR-Cas tools for in vivo genome editing therapy: Trends and challenges. J. Contr. Release *342*, 345–361. https://doi.org/10.1016/j.jconrel.2022.01.013.
30. Kulkarni, J.A., Cullis, P.R., and van der Meel, R. (2018). Lipid Nanoparticles Enabling Gene Therapies: From Concepts to Clinical Utility. Nucleic Acid Therapeut. *28*, 146–157. https://doi.org/10.1089/nat.2018.0721.
31. Lupo, M.G., and Ferri, N. (2018). Angiopoietin-Like 3 (ANGPTL3) and Atherosclerosis: Lipid and Non-Lipid Related Effects. J. Cardiovasc. Dev. Dis. *5*, 39. https://doi.org/10.3390/jcdd5030039.
32. Ye, Z., Bonam, S.R., McKay, L.G.A., Plante, J.A., Walker, J., Zhao, Y., Huang, C., Chen, J., Xu, C., Li, Y., et al. (2023). Monovalent SARS-COV-2 mRNA vaccine using optimal UTRs and LNPs is highly immunogenic and broadly protective against Omicron variants. Proc. Natl. Acad. Sci. USA *120*, e2311752120. https://doi.org/10.1073/pnas.2311752120.
33. Bottger, R., Pauli, G., Chao, P.H., Al Fayez, N., Hohenwarter, L., and Li, S.D. (2020). Lipid-based nanoparticle technologies for liver targeting. Adv. Drug Deliv. Rev. *154–155*, 79–101. https://doi.org/10.1016/j.addr.2020.06.017.

34. Gwon, M.-H., Im, Y.-S., Seo, A.-R., Kim, K.Y., Moon, H.-R., and Yun, J.-M. (2020). Phenethyl Isothiocyanate Protects against High Fat/Cholesterol Diet-Induced Obesity and Atherosclerosis in C57BL/6 Mice. Nutrients *12*, 3657.

35. Bryson, T.E., Anglin, C.M., Bridges, P.H., and Cottle, R.N. (2017). Nuclease-Mediated Gene Therapies for Inherited Metabolic Diseases of the Liver. Yale J. Biol. Med. *90*, 553–566.

36. Nygaard, S., Barzel, A., Haft, A., Major, A., Finegold, M., Kay, M.A., and Grompe, M. (2016). A universal system to select gene-modified hepatocytes in vivo. Sci. Transl. Med. *8*, 342ra79. https://doi.org/10.1126/scitranslmed.aad8166.

37. Wang, J., Zhao, J., Yan, C., Xi, C., Wu, C., Zhao, J., Li, F., Ding, Y., Zhang, R., Qi, S., et al. (2022). Identification and evaluation of a lipid-lowering small compound in preclinical models and in a Phase I trial. Cell Metab. *34*, 667–680.e6. https://doi.org/10.1016/j.cmet.2022.03.006.

38. Pouwer, M.G., Pieterman, E.J., Worms, N., Keijzer, N., Jukema, J.W., Gromada, J., Gusarova, V., and Princen, H.M.G. (2020). Alirocumab, evinacumab, and atorvastatin triple therapy regresses plaque lesions and improves lesion composition in mice. J. Lipid Res. *61*, 365–375. https://doi.org/10.1194/jlr.RA119000419.

39. Finn, J.D., Smith, A.R., Patel, M.C., Shaw, L., Youniss, M.R., van Heteren, J., Dirstine, T., Ciullo, C., Lescarbeau, R., Seitzer, J., et al. (2018). A Single Administration of CRISPR/Cas9 Lipid Nanoparticles Achieves Robust and Persistent In Vivo Genome Editing. Cell Rep. *22*, 2227–2235. https://doi.org/10.1016/j.celrep.2018.02.014.

40. Fiumara, M., Ferrari, S., Omer-Javed, A., Beretta, S., Albano, L., Canarutto, D., Varesi, A., Gaddoni, C., Brombin, C., Cugnata, F., et al. (2024). Genotoxic effects of base and prime editing in human hematopoietic stem cells. Nat. Biotechnol. *42*, 877–891. https://doi.org/10.1038/s41587-023-01915-4.

41. Webber, B.R., Lonetree, C.L., Kluesner, M.G., Johnson, M.J., Pomeroy, E.J., Diers, M.D., Lahr, W.S., Draper, G.M., Slipek, N.J., Smeester, B.A., et al. (2019). Highly efficient multiplex human T cell engineering without double-strand breaks using Cas9 base editors. Nat. Commun. *10*, 5222. https://doi.org/10.1038/s41467-019-13007-6.

42. Khirallah, J., Eimbinder, M., Li, Y., and Xu, Q. (2023). Clinical progress in genome-editing technology and in vivo delivery techniques. Trends Genet. *39*, 208–216. https://doi.org/10.1016/j.tig.2022.12.001.

43. Vekemans, K., and Braet, F. (2005). Structural and functional aspects of the liver and liver sinusoidal cells in relation to colon carcinoma metastasis. World J. Gastroenterol. *11*, 5095–5102. https://doi.org/10.3748/wjg.v11.i33.5095.

44. Zhang, C., Yang, Y., Qi, T., Zhang, Y., Hou, L., Wei, J., Yang, J., Shi, L., Ong, S.-G., Wang, H., et al. (2023). Prediction of base editor off-targets by deep learning. Nat. Commun. *14*, 5358. https://doi.org/10.1038/s41467-023-41004-3.

45. Clement, K., Rees, H., Canver, M.C., Gehrke, J.M., Farouni, R., Hsu, J.Y., Cole, M.A., Liu, D.R., Joung, J.K., Bauer, D.E., and Pinello, L. (2019). CRISPResso2 provides accurate and rapid genome editing sequence analysis. Nat. Biotechnol. *37*, 224–226. https://doi.org/10.1038/s41587-019-0032-3.

46. Bae, S., Park, J., and Kim, J.-S. (2014). Cas-OFFinder: a fast and versatile algorithm that searches for potential off-target sites of Cas9 RNA-guided endonucleases. Bioinformatics *30*, 1473–1475. https://doi.org/10.1093/bioinformatics/btu048.

47. Doman, J.L., Sousa, A.A., Randolph, P.B., Chen, P.J., and Liu, D.R. (2022). Designing and executing prime editing experiments in mammalian cells. Nat. Protoc. *17*, 2431–2468. https://doi.org/10.1038/s41596-022-00724-4.